

## Size effects in submicron exchange bias square elements

G. Vallejo-Fernandez and J. N. Chapman

Citation: [Applied Physics Letters](#) **94**, 262508 (2009); doi: 10.1063/1.3170233

View online: <http://dx.doi.org/10.1063/1.3170233>

View Table of Contents: <http://scitation.aip.org/content/aip/journal/apl/94/26?ver=pdfcov>

Published by the [AIP Publishing](#)

---

### Articles you may be interested in

[Effect of grain cutting in exchange biased nanostructures](#)

J. Appl. Phys. **115**, 17B905 (2014); 10.1063/1.4868328

[Defect mediated tuning of exchange bias in IrMn/CoFe nanostructure](#)

J. Appl. Phys. **105**, 07D722 (2009); 10.1063/1.3072825

[Size effects on the magnetization reversal behavior of exchange bias modulated thin films](#)

J. Appl. Phys. **104**, 013926 (2008); 10.1063/1.2951887

[Characterization and analysis of the training effect of exchange bias in coupled Ni Fe/Ir Mn bilayers](#)

J. Appl. Phys. **101**, 09E513 (2007); 10.1063/1.2709757

[Effect of Ga + ion irradiation on the structural and magnetic properties of CoFe/IrMn exchange biased bilayers](#)

J. Appl. Phys. **95**, 7772 (2004); 10.1063/1.1745120

---

A promotional banner for Applied Physics Reviews. On the left is a small image of the journal cover for 'Applied Physics Reviews', which shows a diagram of a layered structure. The main part of the banner has a blue background with a bright light source on the right. The text 'NEW Special Topic Sections' is written in large, white, sans-serif font. Below this, in orange text, it says 'NOW ONLINE'. Then, in white text, it says 'Lithium Niobate Properties and Applications: Reviews of Emerging Trends'. On the right side, the 'AIP Applied Physics Reviews' logo is displayed in white.

# Size effects in submicron exchange bias square elements

G. Vallejo-Fernandez<sup>a)</sup> and J. N. Chapman

*Department of Physics and Astronomy, University of Glasgow, Glasgow G12 8QQ, United Kingdom*

(Received 21 May 2009; accepted 15 June 2009; published online 2 July 2009)

The behavior of submicron exchange bias square elements has been investigated for systems containing metallic polycrystalline layers. Numerical simulations using a simple theoretical model show that the exchange bias for such elements can increase and/or decrease depending on the microstructure of the antiferromagnetic layer and, in particular, its grain size distribution. The predictions are based on a granular model of exchange bias that accounts for grain cutting at the edges of the nanoelements that takes place during ion milling/etching. This leads to distributions of exchange bias fields that can be quite broad, especially in sub-250 nm elements. © 2009 American Institute of Physics. [DOI: 10.1063/1.3170233]

Exchange bias refers to the shift of the hysteresis loop along the magnetic field axis of systems consisting of a ferromagnetic (F) layer grown in direct contact with an antiferromagnetic (AF) layer.<sup>1</sup> From a technological point of view, it has attracted great attention since the introduction in 1991 of a magnetoresistive read head based on anisotropic magnetoresistance. The implementation of the magnetic tunnel junction sensor in the mid-90s led to the development of magnetic random access memories (MRAM). Although exchange bias has been used in commercial applications for almost two decades, a full understanding of this phenomenon is still missing. The situation becomes more complicated in the nanoscale, where exchange bias in submicron elements has been reported to decrease,<sup>2</sup> and/or increase,<sup>3</sup> when compared to the values measured for thin films. For a recent review of exchange bias in nanostructures, see Ref. 4.

One of the parameters that limits the development of technologies such as MRAM is the fact that the magnetic elements do not all switch at the same field giving rise to a switching field distribution (SFD).<sup>5</sup> The origin of the SFD lies in the fact that lithographic elements can never be produced to have exactly the same size and shape. This situation is further complicated by microstructural variations such as the grain size and orientation within the elements, the anisotropy of the material and, more pertinently, dipole-dipole interactions between the nanoelements, which lead to cross talk.<sup>6</sup>

In this letter, we present a simple numerical model that can account for the experimental features observed in submicron square structures of size  $L$  containing metallic polycrystalline AF layers. Simulations are performed using typical parameters for two of the most important AF materials from a technological point of view: FeMn and IrMn.

Samples produced by sputtering result in wide distributions of grain sizes and, therefore, wide distributions of energy barriers. Recently,<sup>7</sup> an interpretation of the exchange bias phenomenon based on the thermal fluctuation model of Fulcomer and Charap<sup>8</sup> has been proposed. The model treats the AF as an assembly of randomly oriented, noninteracting grains distributed in size. The distribution of grain sizes  $D$  is assumed to be lognormal since that is the case for sputtered thin films. Hence,  $\ln(D)$  is normally distributed with a mean

value  $\mu$  and a standard deviation  $\sigma$ . Each AF grain is assumed to support a single magnetic domain giving an energy barrier of the form,<sup>7</sup>

$$\Delta E = K_{AF} V_{AF} \left[ 1 - \frac{H^*}{H_K^*} \right]^2, \quad (1)$$

where  $V_{AF}$  is the volume of the grain,  $K_{AF}$  is the anisotropy of the AF grain,  $H^*$  is the exchange field from the F layer, which lowers the energy barrier to reversal, and  $H_K^*$  is a pseudoanisotropy field similar to the anisotropy field in single domain ferromagnets. Assuming a uniform value for  $K_{AF}$  at the temperature of measurement we can write:

$$H_{ex}(T) \propto \int_{V_c(T)}^{V_{set}(T_{set})} f(V) dV, \quad (2)$$

where  $H_{ex}(T)$  is the magnitude of the loop shift at the temperature of measurement and  $f(V)$  represents the distribution of grain volumes in the AF. Under ideal conditions there would be an intrinsic value of  $H_{ex}(T)$  which is then moderated by the fraction of the bulk of the AF that contributes to  $H_{ex}$  and also by the strength of the interfacial coupling. The values of  $H_{ex}$  reported in this paper correspond to the contribution to  $H_{ex}$  from the bulk of the AF given by the evaluation of the integral in Eq. (2) and, hence, have no units. Figure 1 shows a schematic diagram of the grain volume distribution within the AF where not the whole AF is aligned with the F layer. Grains with  $V > V_{set}$  remain unaligned due to their anisotropy energy being too large. Moreover, grains with  $V < V_c$  are thermally unstable at the temperature of measurement. Hence, only the grains in the window delimited by  $V_c$  and  $V_{set}$  contribute to the loop shift. The two critical volumes are given by:

$$V_c = \frac{\ln(t_{meas} f_0) k_B T_{meas}}{K_{meas}}, \quad (3)$$

$$V_{set} = \frac{\ln(t_{set} f_0) k_B T_{set}}{K_{set}}, \quad (4)$$

where  $t_{meas}$  is the time of measurement,  $k_B$  is Boltzmann's constant,  $T_{meas}$  is the temperature of measurement,  $K_{meas}$  is the value of the anisotropy at  $T_{meas}$ ,  $t_{set}$  is the setting/annealing time,  $T_{set}$  is the setting temperature, and  $K_{set}$  is the value of the anisotropy at the setting temperature. A tempera-

<sup>a)</sup>Electronic mail: g.fernandez@physics.gla.ac.uk.

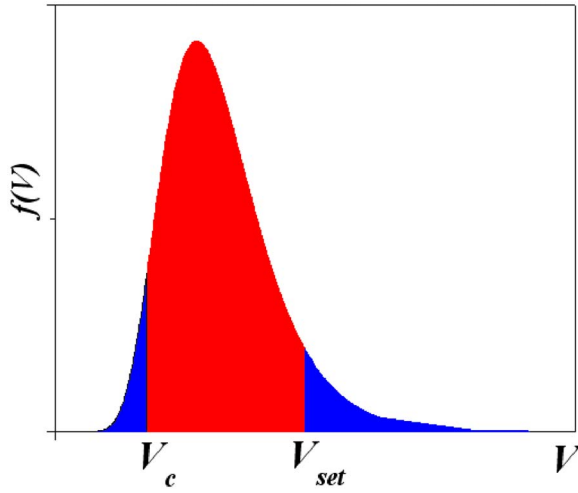


FIG. 1. (Color online) Schematic of the grain volume distribution in the AF after setting a fraction of the AF and cooling to a temperature where some of the smaller AF grains remain thermally unstable.

ture dependence of the form  $(1-T/T_N)$  is assumed for  $K_{AF}$ , where  $T_N$  is the Néel temperature of the AF.<sup>9</sup>

The AF layer is modeled as a granular microstructure following a lognormal distribution with parameters  $\mu$  and  $\sigma$ . For all the calculations presented in this work  $\mu=2.30$  and  $\sigma=0.27$ . The mean grain size in the film is given by  $D_m = e^\mu$  ( $\sim 10$  nm in our simulations). Due to the ion milling/etching process grains at the edges of the nanoelements will be randomly cut leading to an effective grain size distribution, which might differ significantly to that for the thin film. Note that for 125 nm elements, edge grains can account for up to 25% of the total area assuming  $D_m=10$  nm. This suggests that grains that did not contribute to the loop displacement in the thin film might now contribute to the loop shift and vice versa. The effective grain size distribution within a given nanoelement is then calculated. The exchange bias for the nanoelements will be given by evaluation of the integral in Eq. (2) where  $f(V)$  has been modified accordingly.

The effect of the element size  $L$ , assumed to be square, on the exchange field for FeMn based exchange biased systems is shown in Figs. 2 and 3. Figure 2 shows the probability distributions of exchange fields within arrays of nanoelements of different sizes. For each array the distribution is generated after calculating the value of the exchange field for 10 000 nanoelements ensuring good statistics. The parameters used for the simulations are as follows:  $K_{FeMn}(293\text{ K})=1.80 \times 10^4\text{ J/m}^3$ ,<sup>10</sup>  $T_{set}=473\text{ K}$ ,  $t_{set}=5400\text{ s}$ ,  $T_{meas}=293\text{ K}$ , and  $t_{meas}=100\text{ s}$ ,  $f_0=10^9\text{ s}^{-1}$ ,  $T_N=490\text{ K}$ ,  $\mu=2.30$  ( $D_m \sim 10\text{ nm}$ )  $\sigma=0.27$ , and  $t_{AF}=10\text{ nm}$ . These values are chosen based on standard measurement/setting conditions.  $H_{ex}$  increases sharply with increasing element size for  $L \leq 500\text{ nm}$ . For bigger elements, the exchange bias saturates, equalling the value of  $H_{ex}$  for thin films as indicated by the dashed line in Fig. 3. On the other hand, the width of the distribution decreases as the element size increases.

The median exchange bias field for each array as a function of element size is shown in Fig. 3. The error bars correspond to the standard deviation of the distributions in Fig. 2. For element sizes  $< 300\text{ nm}$  distributions as broad as 32% are observed. These results are in excellent agreement with the work of Sasaki *et al.*<sup>2</sup>

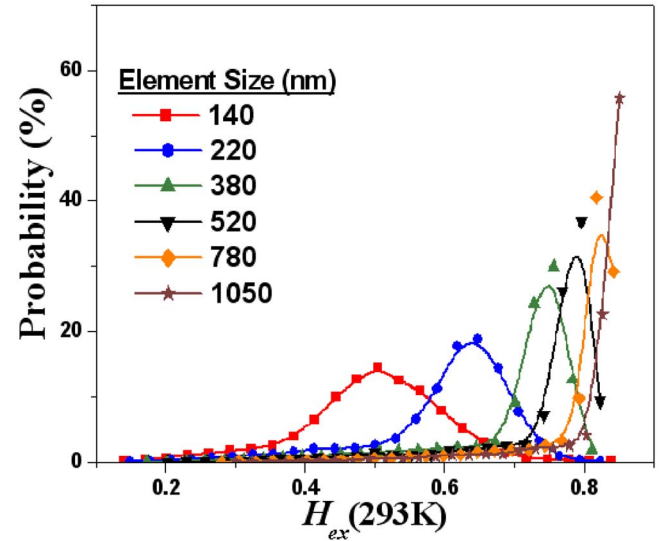


FIG. 2. (Color online) Distribution of exchange bias fields for systems containing an FeMn AF layer as a function of the element lateral size. The lines are guides to the eye.

Similar calculations have been performed assuming parameters typical of IrMn. In this case we have examined the effect of the AF layer thickness on the exchange field at constant element size. For the calculations shown in Figs. 4 and 5,  $K_{IrMn}(293\text{ K})=5.5 \times 10^5\text{ J/m}^3$ ,  $T_{set}=550\text{ K}$ , and  $T_N=690\text{ K}$ .<sup>11</sup> The thickness of the AF layer was varied between 5 and 19 nm while  $L=90\text{ nm}$  in all cases. These values were chosen so the theoretical predictions could be compared to experimental results available in the literature.<sup>3</sup> The other parameters were kept the same as for the FeMn simulations. Figure 4 shows the probability distributions of exchange bias fields as a function of AF thickness. It is clear from this figure that for thick AF layers ( $t_{AF} \geq 10\text{ nm}$ ),  $t_{AF}$  does not have a significant impact on the width of the distribution. However, for thinner samples, an enhancement in the standard deviation of the distribution is observed.

Figure 5 shows the median exchange bias field and standard deviation as a function of AF thickness for the nanoele-

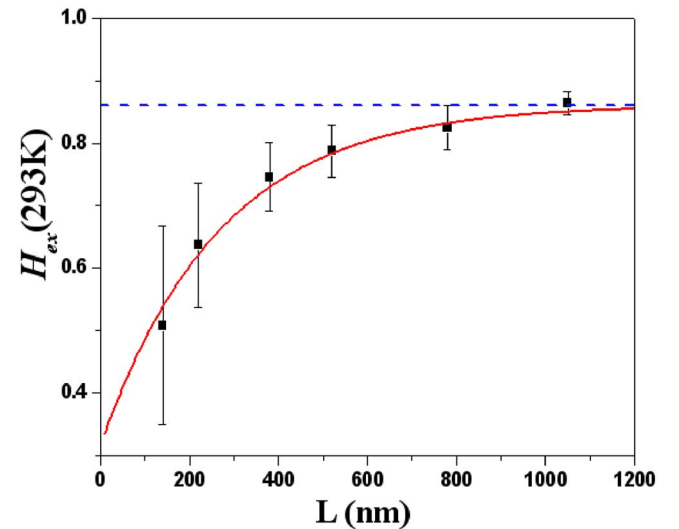


FIG. 3. (Color online) Variation of the median exchange bias field with the element size  $L$  for FeMn exchange biased systems. The line is a guide to the eye.

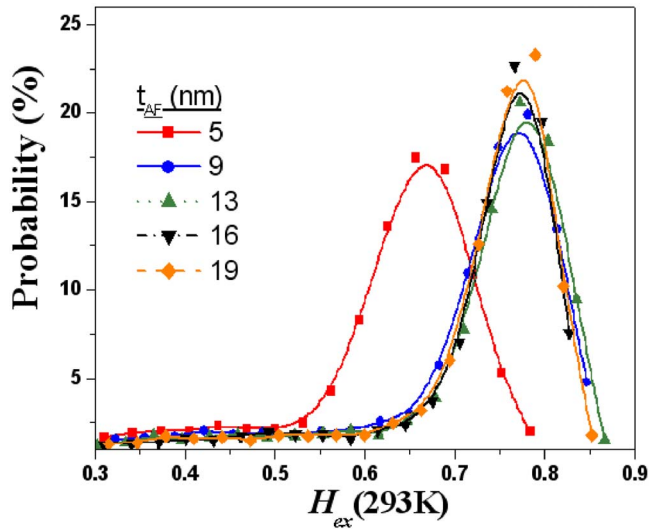


FIG. 4. (Color online) Distribution of exchange bias fields for systems containing an IrMn AF layer as a function of AF thickness for constant element size ( $L=90$  nm). The lines are a guide to the eye.

ments (solid symbols) as well as for thin film samples (empty symbols). For samples with  $t_{AF} > 5$  nm the exchange bias does not vary significantly as a function of  $t_{AF}$  in the patterned samples. Moreover, above  $t_{AF} \sim 10$  nm the exchange bias is higher for the nanoelements. On the other hand, for low AF thicknesses, the exchange bias is higher for the thin films. This is due to the fact that for thick AF layers, a significant fraction of the grains lie outside the window delimited by  $V_c$  and  $V_{set}$ . Increasing the thickness of the AF layer increases the grain volume, not the grain diameter, resulting in a greater fraction of the AF that cannot be set. Upon patterning, some of these grains will be cut resulting in a larger number of grains contributing to the loop shift. These results are in excellent agreement with the work of Baltz *et al.*<sup>3</sup>

In conclusion, we have shown that features observed in submicron metallic polycrystalline exchange bias elements can be explained in terms of a simple granular model that takes into account grain cutting at the edges of the nanoelements. This leads to a wide distribution of exchange bias fields for elements below 250 nm. Control of the AF micro-

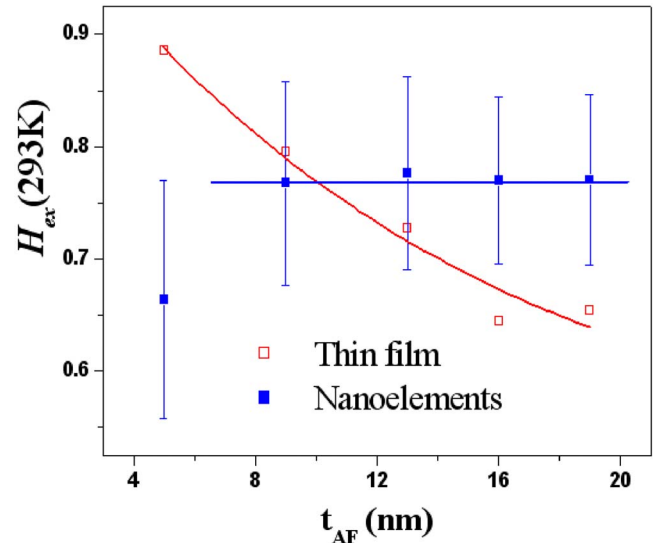


FIG. 5. (Color online) Variation of the exchange bias as a function of the thickness of the AF layer for nanoelements (solid symbols) and thin films (open symbols). The lines are a guide to the eye.

structure can lead to better, i.e., narrower, switching properties. The exchange field can both increase and decrease depending on material parameters, specifically the grain size distribution and anisotropy of the AF material.

<sup>1</sup>W. H. Meiklejohn and C. P. Bean, *Phys. Rev.* **102**, 1413 (1956).

<sup>2</sup>T. Sasaki, R. Nakatani, K. Ishimoto, Y. Endo, Y. Shiratsuchi, Y. Kawamura, and M. Yamamoto, *J. Magn. Magn. Mater.* **310**, 2677 (2007).

<sup>3</sup>V. Baltz, J. Sort, S. Landis, B. Rodmacq, and B. Dieny, *Phys. Rev. Lett.* **94**, 117201 (2005).

<sup>4</sup>J. Nogues, J. Sort, V. Langlais, V. Skumryev, S. Suriñach, J. S. Muñoz, and M. D. Baro, *Phys. Rep.* **422**, 65 (2005).

<sup>5</sup>W.C. Jeong, J.H. Park, G.H. Koh, G.T. Jeong, H.S. Jeong, and K. Kim, *J. Appl. Phys.* **97**, 10C905 (2005).

<sup>6</sup>X. Zhu, P. Grütter, Y. Hao, F. J. Castaño, S. Haratani, and C. A. Ross, *J. Appl. Phys.* **93**, 1132 (2003).

<sup>7</sup>G. Vallejo-Fernandez, L. E. Fernandez-Outon, and K. O'Grady, *J. Phys. D: Appl. Phys.* **41**, 112001 (2008).

<sup>8</sup>E. Fulcomer and S. H. Charap, *J. Appl. Phys.* **43**, 4190 (1972).

<sup>9</sup>M. D. Stiles and R. D. McMichael, *Phys. Rev. B* **60**, 12950 (1999).

<sup>10</sup>L. E. Fernandez-Outon, G. Vallejo-Fernandez, S. Manzoor, B. Hillbrands, and K. O'Grady, *J. Appl. Phys.* **104**, 093907 (2008).

<sup>11</sup>G. Vallejo-Fernandez, L. E. Fernandez-Outon, and K. O'Grady, *Appl. Phys. Lett.* **91**, 212503 (2007).